Pattern Recognition Letters 112 (2018) 332–339

Contents lists available at ScienceDirect

Pattern Recognition Letters

journal homepage: www.elsevier.com/locate/patrec

Some computational aspects of Tchebichef moments for higher orders

César Camacho-Bello*, José S. Rivera-Lopez

Universidad Politécnica de Tulancingo, Hidalgo, México

ARTICLE INFO

Article history:
Received 18 September 2017
Available online 13 August 2018

Keywords:
Discrete orthogonal polynomials
Tchebichef polynomials
Tchebichef moments
Recurrence algorithm
Numerical propagations errors

ABSTRACT

In this work, we propose a new algorithm for the computation of Tchebichef moments by means of a recurrence relation with respect to order and the Gram–Schmidt process, which reduces the numerical instability and the carry error caused by the computation of high-order moments. Results and comparison with other methods are presented.

1. Introduction

Tchebichef (Chebyshev) moments have been extensively used in the field of image analysis and pattern recognition. Mukundan et al. [18] introduced for the first time the moments of Tchebichef. The use of Tchebichef polynomials as kernel of moments, which eliminate the need for numerical approximation, satisfy the orthogonal condition in discrete domain of digital image [15,17,18]. The Tchebichef moments are used in many applications such as: image watermarking [4,12,29], feature invariants in pattern recognition [19,28,31], vehicle logo recognition [20], image compression [7,16,21], speech recognition [5,6], image restoration [23,27], human action recognition [13], facial recognition [3], medical image registration [26], and texture-based image recognition [2].

Mukundan et al. [18] discuss some computational aspects of Tchebichef polynomials and moments, such as symmetry property, polynomial expansion, and recurrence relations with respect to n and x. However, one problem encountered in the calculation of high-order polynomial values is the propagation of numerical error while using the recursive relation with respect to n [30]. The recursive procedure used for polynomial evaluation can be suitably modified to reduce the accumulation of numerical error with the recurrence relation in x-direction proposed by Mukundan [15].

From the recurrence relations different strategies have been developed for the computation of Tchebichef moments. Wang and Wang [24] used Clenshaws recurrence formula to develop recursive algorithms for the computation of the forward and inverse Tchebichef moments. Kotoulas and Andreadis [11] present a hardware architecture using FPGA which enables real-time processing of binary and grayscale images. Shu et al. [22] propose a new approach for fast computation through image block representation for binary image and intensity slice representation for grayscale images. Honarvar et al. [9] derive a simplified recurrence relationship to compute Tchebichef polynomials based on Z-transform properties. Recently, Abdulhussain et al. [1] propose a new method for computing high order moments, their algorithm is based on the integration in a sequential manner of two traditional recurrence relations (the x-direction and the n-direction algorithms) proposed by Mukundan [15]. Even so, the orthogonality of Tchebichef polynomials for higher orders is destroyed because of numerical approximation. This problem severely affects the quality of image reconstruction particularly in high resolution images. A solution can be devised to eliminate the carry error to compute high-order polynomials through the Gram–Schmidt process. On the other hand, to quantify the orthogonality error of the Tchebichef polynomials, we propose to use the universal quality index in order to know the size N and the order n that satisfies the orthogonality condition.

2. Tchebichef polynomials

The classical orthogonal polynomials are characterized by being solutions of the differential equation of the hypergeometric type defined as

$$0 = \sigma(x)\Delta\nabla t_n(x;N) + \tau(x)\Delta t_n(x;N) + \lambda_n \tag{1}$$

where $\Delta t_n(x;N) = t_n(x+1;N) - t_n(x;N)$, $\nabla t_n(x;N) = t_n(x;N) - t_n(x-1;N)$ denote the forward and backward finite difference operator, respectively. Hence $\Delta\nabla t_n(x;N) = t_n(x+1;N) - 2t_n(x;N) + t_n(x-1;N)$. Finally, $\sigma(x)$ and $\tau(x)$ are polynomials of at most

* Corresponding author.
E-mail address: cesar.camacho@upt.edu.mx (C. Camacho-Bello).

https://doi.org/10.1016/j.patrec.2018.08.020
0167-8655/

the second and first degree, and λ_n is a constant. The variation on their values can form various types of orthogonal polynomials such as: Tchebichef, Mexnier, Kravchuk, Charlier, Hahn, dual Hahn and Racah polynomials. The initial values of the Tchebichef polynomials are given by,

$$\sigma(x) = x(N-x) \tag{2}$$

$$\tau(x) = N-1-2x \tag{3}$$

$$\lambda_n = n(n+1) \tag{4}$$
$$\forall n, x = 0,1,2,\ldots,N-1$$

where n is order of the polynomial and N is the discrete domain of the polynomial. The solution of the differential equation can be defined by the hypergeometric function,

$$t_n(x;N) = (1-N)_n {}_3F_2(-n,-x.1+n;1,1-N;1) \tag{5}$$

where $(\cdot)_k$ is the Pochhammer symbol given by

$$(a)_k = a(a+1)(a+2)\ldots(a+k-1). \tag{6}$$

The ${}_3F_2(\cdot)$ is the generalized hypergeometric function, defined as

$${}_3F_2(-n,-x.1+n;1,1-N;1) = \sum_{k=0}^{\infty}\frac{(-n)_k(-x)_k(1+n)_k}{(1)_k(1-N)_k k!}. \tag{7}$$

The set of $t_n(x;N)$ satisfies the following orthogonality condition,

$$\sum_{x=0}^{N-1} t_n(x;N)t_m(x;N)\varrho(x) = \delta_{nm}d_n^2 \tag{8}$$

where δ_{nm} is the Kronecker delta, $\varrho(x)$ is the weight, and d_n^2 is the squared norm, defined as

$$\delta_{nm} = \begin{cases} 1, & n=m \\ 0, & n \neq m. \end{cases} \tag{9}$$

$$\varrho(x) = 1, \tag{10}$$

$$d_n^2 = \frac{(N+n)!}{(2n+1)(N-n-1)!} \tag{11}$$

Therefore, the Tchebichef polynomials orthonormalized are defined as follows

$$t_n(x;N) = \sqrt{\frac{\varrho(x)}{d_n^2}}(1-N)_n {}_3F_2(-n,-x.1+n;1,1-N;1) \tag{12}$$

Moreover, the symmetry property of the Tchebichef polynomials reduces the computation time, which is defined as follows

$$t_n(N-1-x;N) = (-1)^n t_n(x;N) \tag{13}$$

3. The recurrence algorithms

Mukundan [15] and Zhu et al. [30] propose to use recurrence relations to reduce numerical instability. Recurrence relations can be calculated in two directions: in the direction of n order and in the direction of x variable. In this section we present a review of recurrence relation with respect to n and to x proposed by Mukundan [15] and Zhu et al. [30], as well as the method of Abdulhussain et al. [1] that is a combination of both. Also, a recurrence relation simplified with respect to n is proposed.

3.1. Recurrence relation with respect to n

Mukundan [15] proposes the following three-term recurrence relation,

$$t_n(x;N) = \alpha_1 x t_{n-1}(x;N) + \alpha_2 t_{n-1}(x;N) + \alpha_3 t_{n-2}(x;N) \tag{14}$$

where

$$\alpha_1 = \frac{2}{n}\sqrt{\frac{4n^2-1}{N^2-n^2}}$$
$$\alpha_2 = \frac{1-N}{n}\sqrt{\frac{4n^2-1}{N^2-n^2}}$$
$$\alpha_3 = \frac{n-1}{n}\sqrt{\frac{2n+1}{2n-3}}\sqrt{\frac{N^2-(n-1)^2}{N^2-n}}$$

On the other hand, Zhu et al. [30] propose two general forms for obtaining classical orthogonal polynomials, which include the Tchebichef polynomials. The general form for recurrence relation with respect to n, is given by

$$At_n(x;N) = B\cdot Dt_{n-1}(x;N) + C\cdot Et_{n-2}(x;N) \tag{15}$$

where

$$A = \frac{n}{2(2n-1)}$$
$$B = x - \frac{N-1}{2}$$
$$C = -\frac{(n-1)\left[N^2-(n-1)^2\right]}{2(2n-1)}$$
$$D = \sqrt{\frac{(2n+1)}{\left(N^2-n^2\right)(2n-1)}}$$
$$E = \sqrt{\frac{2n+1}{\left(N^2-n^2\right)\left[N^2-(n-1)^2\right](2n-3)}}$$

It is easy to see that the coefficients of the recurrence relation of three terms can be algebraically reduced. In this paper we propose the simplification of Eq. (15), which is given by,

$$\omega_n t_n(x;N) = \omega t_{n-1}(x;N) - \omega_{n-1}t_{n-2}(x;N) \tag{16}$$

where

$$\omega = 2x-N+1$$
$$\omega_n = n\sqrt{\frac{N^2-n^2}{(2n+1)(2n-1)}}$$

Note that ω has to be calculated once and remains constant when we calculate each n order, while ω_n depends on n.

For the initial numerical calculation, Tchebichef polynomials of zero-order and first-order are given by

$$t_0(x;N) = \frac{1}{\sqrt{N}} \tag{17}$$

$$t_1(x;N) = (2x-N+1)\sqrt{\frac{3}{N\left(N^2-1\right)}} \tag{18}$$

The initial conditions are the same for the Eqs. (14)–(16).

3.2. Recurrence relation with respect to x

Mukundan [15] proposes the three-term recurrence algorithm in the x-direction is defined as

$$t_n(x;N) = \beta_1 t_n(x-1;N) + \beta_2 t_n(x-2;N) \tag{19}$$

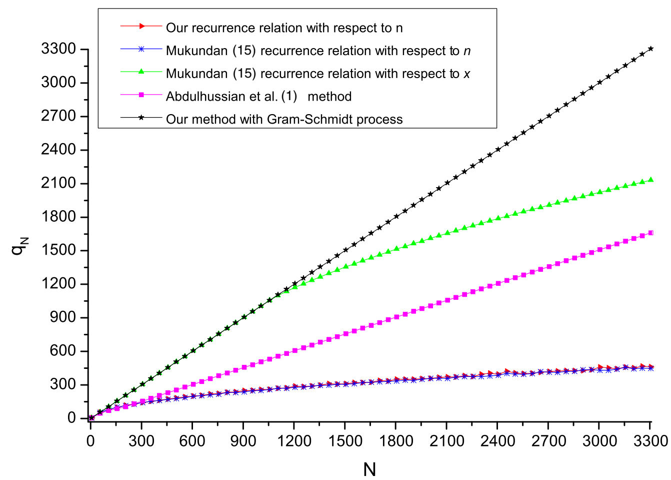

Fig. 1. Orthogonality test of different recurrence relations with size N.

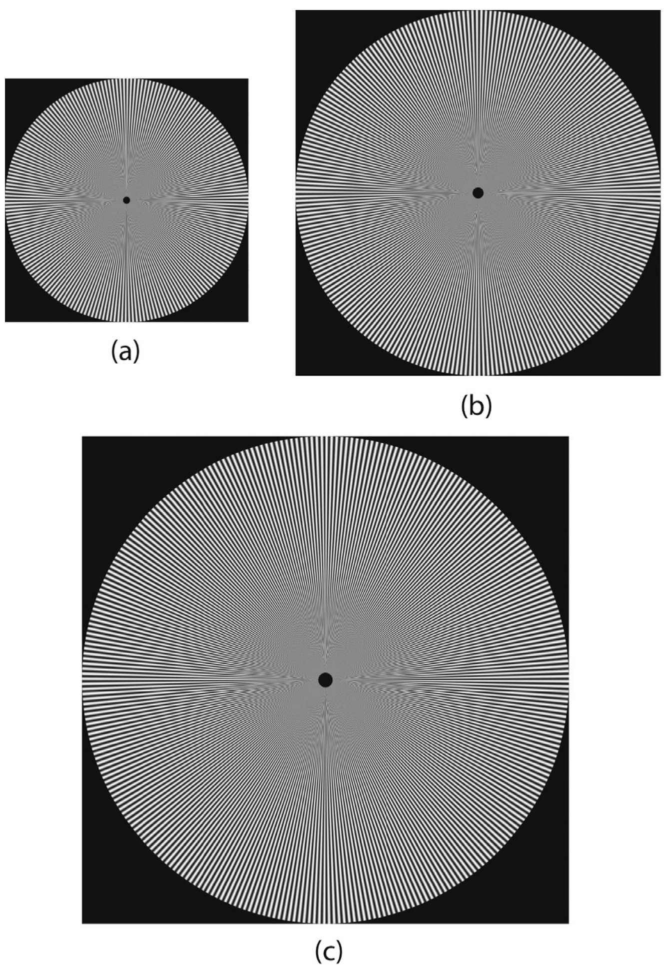

Fig. 2. Resolution of test images: (a) 4000×4000 px, (b) 6000×6000 px, and (c) 8000×8000 px. Number of cycles: (a) $\omega = 200$, (b) $\omega = 250$, and (c) $\omega = 300$.

where

$$\beta_1 = \frac{-n(n+1) - (2x-1)(x-N-1) - x}{x(N-x)}$$
$$\beta_2 = \frac{(x-1)(x-N-1)}{x(N-x)}$$

Moreover, Zhu et al. [30] propose a general form for obtaining Tchebichef polynomials whit respect to x, which are given by

$$t_n(x;N) = \frac{\sqrt{\varrho(x)}}{\sigma(x-1)+\tau(x-1)}\left[\frac{2\sigma(x-1)+\tau(x-1)-\lambda_n}{\sqrt{\varrho(x-1)}}\right.$$
$$\left.\times\, t_n(x-1;N) - \frac{\sigma(x-1)}{\sqrt{\varrho(x-2)}}t_n(x-2;N)\right] \tag{20}$$

The initial values for the recurrence relations can be obtained by

$$t_0(0;N) = \frac{1}{\sqrt{N}}$$
$$t_n(0;N) = -\sqrt{\frac{N-n}{N+n}}\sqrt{\frac{2n+1}{2n-1}}t_{n-1}(0;N)$$
$$t_n(1;N) = \left(1 + \frac{n(1+n)}{1-N}\right)t_n(0;N)$$

3.3. Three-term recurrence algorithm for higher polynomial order

Abdulhussain et al. [1] proposed an algorithm, which is based on the integration of the recurrence relation with respect to x and respect to n in sequential manner. The three-term recurrence algorithm for higher polynomial order is given by Eq. (21) where $l_x = N/2 - \sqrt{(N/2)^2 - (n/2)^2}$. The values for the second half of the polynomial array where $n = 0, 1, \ldots, N-1$ and $x = N/2, N/2+1, \ldots, N-1$ are obtained using the symmetry condition property defined by Eq. (13).

$$t_n(x;N) = \begin{cases} \beta_1 t_n(x-1;N) + \beta_2 t_n(x-2;N) \\ \quad \text{for } 0 \le n < N/2-1 \text{ and } 2 < x < N/2-1 \\ \alpha_1 x t_{n-1}(x;N) + \alpha_2 t_{n-1}(x;N) + \alpha_3 t_{n-2}(x;N) \\ \quad \text{for } N/2 \le n < N-1 \text{ and } l_x < x < N/2-1 \\ \beta_1 t_n(x-1;N) + \beta_2 t_n(x-2;N) \\ \quad \text{for } N/2 \le n < N-1 \text{ and } l_x - 12 < x < l_x \end{cases} \tag{21}$$

4. Tchebichef moments

Tchebichef moments $T_{n,\,m}$ of an image $f(x, y)$ of size $N \times M$ are a set of orthogonal moments, which can be defined by

$$\phi_{n.m} = \sum_{x=0}^{N-1}\sum_{y=0}^{M-1} t_n(x;N)t_m(x;M)f(x,y) \tag{22}$$

where $n = 0, 1, 2, \ldots N-1$ and $m = 0, 1, 2, \ldots, M-1$. In matrix form, the Tchebichef moments matrix, $\mathbf{Q}$, is defined as

$$\mathbf{Q} = \mathbf{T}_1\mathbf{A}\mathbf{T}_2' \tag{23}$$

where $(')$ denotes the transpose of the matrix and

$$\mathbf{Q} = \left\{Q_{j,i}\right\}_{i,j=0}^{i=M-1,\,j=N-1}$$
$$\mathbf{T}_1 = \{t_n(x;N)\}_{i,j=0}^{i,j=N-1}$$
$$\mathbf{T}_2 = \{t_m(y;M)\}_{i,j=0}^{i,j=M-1}$$
$$\mathbf{A} = \{f(x,y)\}_{i,j=0}^{i=M-1,\,j=N-1} \tag{24}$$

According to orthogonal theories, the image function $f(x, y)$ can be written completely in terms of the Tchebichef moments. The reconstructed discrete distribution of the image is given by

$$\tilde{f}(x,y) = \sum_{n=0}^{N-1}\sum_{m=0}^{M-1} t_n(x;N)t_m(x;M)\phi_{n.m} \tag{25}$$

where $\tilde{f}(x,y)$ is the reconstructed version of $f(x, y)$. Image reconstruction can help to determine how well an image may be characterized by a small finite set of its moments. Also, the image can

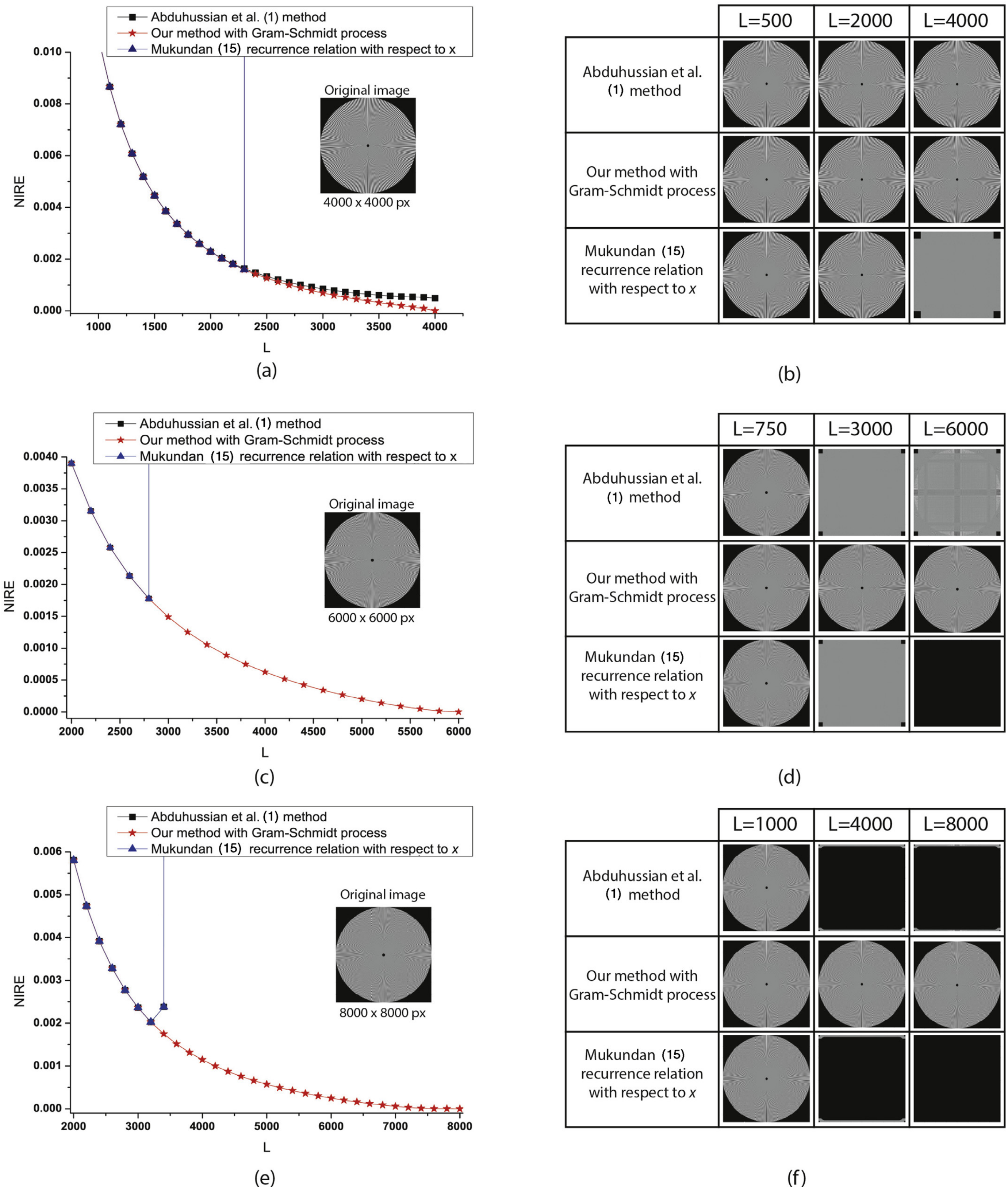

Fig. 3. Comparative analysis of NIRE with different resolutions: (a) 4000×4000 px, (c) 6000×6000 px, and (e) 8000×8000 px. Image reconstruction with different resolutions: (b) 4000×4000 px, (d) 6000×6000 px, and (f) 8000×8000 px.

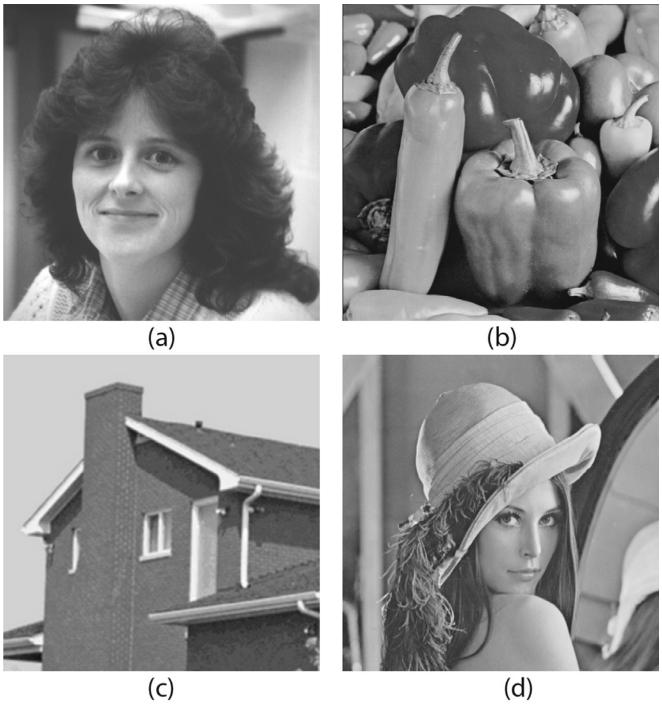

Fig. 4. Reconstruction of standard images with the mega-scale size of 8000×8000 pixels. (a) Dark-hair woman ($NIRE = 4.8155 \times 10^{-29}$ with 8000×8000 moments). (b) Pepper ($NIRE = 4.959 \times 10^{-29}$ with 8000×8000 moments). (c) House ($NIRE = 4.8258 \times 10^{-29}$ with 8000×8000 moments). (b) Lena ($NIRE = 4.7983 \times 10^{-29}$ with 8000×8000 moments).

be reconstructed in the matrix form,

$$\mathbf{A} = \mathbf{T}_1' \mathbf{Q} \mathbf{T}_2. \tag{26}$$

5. Orthonormalization of the Tchebichef polynomials with Gram–Schmidt process

The kernel of Tchebichef moments is calculated by recurrence relations, which leads to propagation and accumulation of rounding-off errors for the calculation of high order moments and large images. In optics, Gram–Schmidt process is commonly used to correct errors in wavefront expansion with Zernike polynomials [14]. In this work a similar approach is taken to correct the numerical instability of the high-order Tchebichef moments. The kernel orthonormalization of the Tchebichef moments is given by Algorithm 1.

Note that in Algorithm 1, we use the recurrence relation of Eq. (16). The proposed recurrence relation is much easier to implement because it has fewer operations than the other recurrence relations with respect to n.

6. Orthogonality preservation

The preservation of the orthogonality condition in orthogonal moments ensures that the descriptors or moments are linearly independent and do not have information redundancy. The orthogonality condition can be expressed by the matrix form given by,

$$\widetilde{\mathbf{I}} = \mathbf{T}_1 \mathbf{T}_2' \tag{27}$$

where $\widetilde{\mathbf{I}}$ is the identity matrix. In order to estimate the structural similarity between the identity matrix and the obtained with the Tchebichef polynomials, we can calculate the universal quality index (*UQI*). This index is designed by modeling any image distortion as a combination of three factors: loss of correlation, luminance distortion, and contrast distortion [25]. For a matrix $\widetilde{\mathbf{I}}$ of size $N \times N$, *UQI* is defined,

$$UQI = \frac{4\sigma_{kp}\mu_k\mu_p}{\left(\mu_k^2 + \mu_p^2\right)\left(\sigma_k^2 - \sigma_p^2\right)} \tag{28}$$

where μ_k and μ_p are the mean matrix values for identity matrix and the matrix obtained from Eq. (27), σ_k and σ_p are the standard deviation for identity matrix ($\mathbf{I}_{i,j}$) and the matrix ($\widetilde{\mathbf{I}}_{i,j}$), finally, σ_{kp} is calculated as

$$\sigma_{kp} = \frac{1}{N^2 - 1} \sum_{i=0}^{N-1} \sum_{j=0}^{N-1} \left[\mathbf{I}_{i,j} - \mu_k\right]\left[\widetilde{\mathbf{I}}_{i,j} - \mu_p\right]. \tag{29}$$

The dynamic range of Q is $[-1, 1]$, the higher value of Q indicates a higher degree of structural similarity. Therefore, polynomials meet the orthogonality condition when $Q \approx 1$. The orthogonality test of moment kernel is defined by Algorithm 2.

Algorithm 1 Orthonormalization of the Tchebichef polynomials with Gram–Schmidt process.

$w \leftarrow 2x - N + 1 \forall x = 0, 1, 2, \ldots, N-1$
$w_1 \leftarrow \sqrt{\frac{N^2-1}{3}}$
$t_0(x; N) \leftarrow \frac{1}{\sqrt{N}}$
$t_1(x; N) \leftarrow \frac{w}{w_1} t_0(x; N)$
for $n = 2$ to $N-1$ **do**
  $w_2 \leftarrow n\sqrt{\frac{N^2-n^2}{(2n+1)(2n-1)}}$
  $t_{n+1}(x; N) \leftarrow \frac{w}{w_2} t_n(x; N) - \frac{w_1}{w_2} t_{n-1}(x; N)$
  $w_1 \leftarrow w_2$
  $T(x; N) \leftarrow t_{n+1}(x; N)$
  for $k = 0$ to n **do**
    $t_{n+1}(x; N) \leftarrow t_{n+1}(x; N) - \left[\sum_{x=0}^{N-1} T(x; N) t_k(x; N)\right] \times t_k(x; N)$
  end for
  $h \leftarrow \sqrt{\sum_{x=0}^{N-1} \left[t_{n+1}(x; N)\right]^2}$
  $t_{n+1}(x; N) \leftarrow \frac{t_{n+1}(x; N)}{h}$
end for

Algorithm 2 Orthogonality test.

$Error \leftarrow 0.99999$
for $N = 0$ to H **do**
  $UQI \leftarrow 1$
  $n \leftarrow 1$
  $\mathbf{T} = \{t_n(x; N)\}_{i,j=0}^{i,j=N-1}$
  while and($UQI > Error, n < N$) **do**
    $n \leftarrow n + 1$
    $\widetilde{\mathbf{I}} \leftarrow \mathbf{T}_{i,j} \mathbf{T}'_{i,j} \begin{matrix} \forall i = 0, 1, 2, \ldots, N-1 \\ \forall j = 0, 1, 2, \ldots, n \end{matrix}$
    $UQI \leftarrow \frac{4\sigma_{kp}\mu_k\mu_p}{(\mu_k^2+\mu_p^2)(\sigma_k^2-\sigma_p^2)}$
  end while
  $q_N \leftarrow n$
end for

The Tchebichef polynomials can be calculated with the different recurrence relations. However, if the calculation of the Tchebichef polynomials is correct, q_n is a straight line, i.e., $q_N = N$. Fig. 1 shows the values of q_N for different recurrence relations. Also, it can be observed that the Tchebichef polynomials calculated with Gram–Schmidt process satisfy the orthogonality condition. Table 1 shows the limit values q_N and q_M of the different recurrence relations that meet the orthogonality condition for different resolutions.

Table 1
Limit values q_N and q_M for different methods and resolutions.

Method	Megapixels	Resolution $N \times M$	q_N	q_M
Our recurrence relation with respect to n	1	1280 × 960	288	252
	2	1600 × 1200	321	278
	3	2048 × 1336	359	298
	4	2240 × 1680	384	335
	5	2560 × 1920	401	352
	6	3000 × 2000	447	352
	7	3072 × 2304	438	392
	8	3264 × 2448	463	394
Mukundan [15] respect to n	1	1280 × 960	291	278
	2	1600 × 1200	319	271
	3	2048 × 1336	351	296
	4	2240 × 1680	379	324
	5	2560 × 1920	395	346
	6	3000 × 2000	434	352
	7	3072 × 2304	441	376
	8	3264 × 2448	444	388
Mukundan [15] respect to x	1	1280 × 960	1267	957
	2	1600 × 1200	1407	1163
	3	2048 × 1336	1630	1256
	4	2240 × 1680	1716	1448
	5	2560 × 1920	1849	1568
	6	3000 × 2000	2020	1605
	7	3072 × 2304	2044	1743
	8	3264 × 2448	2114	1804
Abduhussian et al. [1] method	1	1280 × 960	642	482
	2	1600 × 1200	804	602
	3	2048 × 1336	1028	672
	4	2240 × 1680	1124	843
	5	2560 × 1920	1284	963
	6	3000 × 2000	1505	1004
	7	3072 × 2304	1540	1156
	8	3264 × 2448	1638	1229
Our method with Gram-Schmidt process	1	1280 × 960	1280	960
	2	1600 × 1200	1600	1200
	3	2048 × 1336	2048	1336
	4	2240 × 1680	2240	1680
	5	2560 × 1920	2560	1920
	6	3000 × 2000	3000	2000
	7	3072 × 2304	3072	2304
	8	3264 × 2448	3264	2448

Table 2
Average computation time of moments for four standard images (dark-hair woman, pepper, house and Lena) with different mega-scale size.

Method	Moments	Resolution 1000 × 1000 px	Resolution 2000 × 2000 px	Resolution 4000 × 4000 px	Resolution 8000 × 8000 px
Our recurrence relation r with respect to n	50 × 50	0.0066s	0.0162s	0.0508s	0.17530s
	100 × 100	0.0120s	0.0278s	0.0931s	0.31860s
	200 × 200	0.0260s	0.0614s	0.1932s	0.65539s
Mukundan [15] respect to n	50 × 50	0.0075s	0.0178s	0.0556s	0.17566s
	100 × 100	0.0130s	0.0323s	0.0869s	0.32890s
	200 × 200	0.0294s	0.0603s	0.1998s	0.65382s
Mukundan [15] respect to x	50 × 50	0.0102s	0.0227s	0.0616s	0.20462s
	100 × 100	0.0179s	0.0453s	0.1131s	0.37035s
	200 × 200	0.0373s	0.0836s	0.2307s	0.74858s
Our method with Gram–Schmidt process	50 × 50	0.0196s	0.0434s	0.1019s	0.27035s
	100 × 100	0.0614s	0.1213s	0.3218s	0.73763s
	200 × 200	0.1829s	0.4374s	1.1195s	2.5563s
Shu et al. [22] method	50 × 50	20.3743s	75.5767s	274.9019s	1003.9s
	100 × 100	48.6296s	152.5524s	460.0353s	1423.2s
	200 × 200	96.1680s	281.4589s	766.5941s	2144.1s

7. Experimental results

This section presents the performance evaluation of the proposed method used to validate the theoretical framework presented above. Sinusoidal Siemens star is used to test the resolution of optical systems. It consists of a pattern of sinusoidal oscillations in a polar coordinate system such that the spatial frequency varies for concentric circles of different sizes and is defined as [8],

$$I(\theta) = a + b\sin(\omega\theta - \phi), \tag{30}$$

where a represents the mean intensity value, b is the amplitude of the intensity oscillations, ω is the integer number of cycles within

Table 3
Comparison of execution-time ratio improvement between our proposed recurrence relation with respect to n and other methods.

Method	Moments	Resolution 1000 × 1000 px	Resolution 2000 × 2000 px	Resolution 4000 × 4000 px	Resolution 8000 × 8000 px
Mukundan [15] respect to n	50 × 50	12.00%	8.99%	8.63%	0.20%
	100 × 100	7.69%	13.93%	7.13%	3.13%
	200 × 200	11.56%	1.82%	3.30%	0.24%
Mukundan [15] respect to x	50 × 50	35.29%	28.63%	17.53%	14.33%
	100 × 100	32.96%	38.63%	17.68%	13.97%
	200 × 200	30.29%	26.55%	16.25%	12.45
Shu et al. [22] method	50 × 50	99.97%	99.98%	99.98%	99.98%
	100 × 100	99.97%	99.98%	99.98%	99.98%
	200 × 200	99.97%	99.98%	99.97%	99.97%

the complete 2π radians of the star, and ϕ is the potential phase offset. In this work, we can use Eq. (30) to measure the spatial frequency response of image reconstruction. For the comparative analysis, $a = 0,\ b = 255$, $\phi = 0$ and $\omega = 200, 250, 300$ are considered for the three test images, which are shown in Fig. 2.

The spokes of sinusoidal Siemens star never touch, the gaps between them become narrower, except in the center. However, when image reconstruction is limited, the spokes appear to touch at some distance from the center. Therefore, a greater number of frequencies or high orders are required to reconstruct the center of the star.

To quantify the performance of the proposed method the normalized image reconstruction error (NIRE) is used. It is defined as the normalized mean square error between the original image $f(x, y)$ and its reconstruction $\tilde{f}(x, y)$, and in discrete form is given by

$$NIRE = \frac{\sum_{x=0}^{N-1}\sum_{y=0}^{M-1}\left[f(x,y) - \tilde{f}(x,y)\right]^2}{\sum_{x=0}^{N-1}\sum_{y=0}^{M-1} f^2(x,y)} \tag{31}$$

On the other hand, image reconstruction can help to establish the feature representation capability of Tchebichef moments by a small finite set of its moments. The results in term of *NIRE* and image reconstruction with the different recurrence relation are shown in Fig. 3.

The proposed method has the ability to reconstruct the image with close to zero errors. Fig. 4 shows the reconstruction of four standard images with mega-scale size.

In terms of execution-time, the proposed method has high computational costs because it is a complex process to correct numerical instability through the Gram–Schmidt orthonormalization process. However, the computation times of the proposed method using the matrix form by Eq. (23) and software specialized in matrix operations have better performance than the fast computation of Tchebichef moments proposed by Shu et al. [22]. Table 2 shows the average time of four standard images using different recurrence relations and the rapid computation proposed by Shu et al. [22]. On the other hand, our recurrence relation with respect to n presents a better execution-time than the different methods. The execution-time improvement ratio (ETIR) is used as criterion to compare the different computation methods [10]. It is defined as follows

$$ETIR = \left(1 - \frac{Time_1}{Time_2}\right) * 100 \tag{32}$$

where $Time_1$ and $Time_2$ are the execution-time of the first and second methods. The execution-time ratio improvement of the moments with our proposed recurrence relation with respect to n is shown in Table 3. The algorithms were implemented in MATLAB edition R2016a on a PC Intel(R) Core(TM) i7-6500U 2.50Hz, 8GB RAM.

8. Conclusions

In this paper, we have presented a new recurrence algorithm to compute the kernel of Tchebichef moments. The proposed method is based on orthonormalization the Tchebichef polynomials using the Gram–Schmidt process. In addition, algebraic simplification of the three-term recurrence relations used in the Gram–Schmidt process helps to reduce numerical instability and computation times. The proposed algorithm can generate the Tchebichef polynomials for large lengths and higher orders. We have also analyzed the importance of preserving orthogonality. The orthogonality test is an important factor in the development of real-world pattern recognition applications; it guarantees that the descriptors or moments are linearly independent with minimal redundant information. Experimental results conclusively prove the effectiveness of the recurrence relations, used in the Gram–Schmidt process, in computing the kernel of Tchebichef moments. The proposed method has been used for image reconstruction and this effectively illustrates its descriptive capacity with respect to other methods.

Acknowledgments

We extend our gratitude to the reviewers and Jennifer Speier for their useful suggestions.

References

[1] S.H. Abdulhussain, A.R. Ramli, S.A.R. Al-Haddad, B.M. Mahmmod, W.A. Jassim, On computational aspects of tchebichef polynomials for higher polynomial order, IEEE Access 5 (2017) 2470–2478.
[2] M. Cheong, K.-S. Loke, An approach to texture-based image recognition by deconstructing multispectral co-occurrence matrices using tchebichef orthogonal polynomials, in: Pattern Recognition, 2008. ICPR 2008. 19th International Conference on, IEEE, 2008, pp. 1–4.
[3] S.D. Dasari, S. Dasari, Face recognition using tchebichef moments, Int. J. Inf. Network Secur. 1 (4) (2012) 243.
[4] C. Deng, X. Gao, X. Li, D. Tao, A local tchebichef moments-based robust image watermarking, Signal Process. 89 (8) (2009) 1531–1539.
[5] F. Ernawan, N.A. Abu, Efficient discrete tchebichef on spectrum analysis of speech recognition, Int. J. Mach. Learn. Comput. 1 (1) (2011) 1.
[6] F. Ernawan, N.A. Abu, N. Suryana, Spectrum analysis of speech recognition via discrete tchebichef transform, in: International Conference on Graphic and Image Processing (ICGIP 2011), 8285, 2011. 82856L–82856L–8
[7] F. Ernawan, N.A. Abu, N. Suryana, An optimal tchebichef moment quantization using psychovisual threshold for image compression, Adv. Sci. Lett. 20 (1) (2014) 70–74.
[8] J.C.G. Gabriel C. Birch, Sinusoidal siemens star spatial frequency response measurement errors due to misidentified target centers, Opt. Eng. 54 (2015). 54–54–8.
[9] B.S.A. Honarvar, R. Paramesran, C.-L. Lim, The fast recursive computation of tchebichef moment and its inverse transform based on z-transform, Digit Signal Process 23 (5) (2013) 1738–1746.
[10] K.M. Hosny, Fast computation of accurate zernike moments, J. Real-Time Image Process. 3 (1) (2008) 97–107.
[11] L. Kotoulas, I. Andreadis, Fast computation of chebyshev moments, IEEE Trans. Circuits Syst. Video Technol. 16 (7) (2006) 884–888.
[12] Z. Li, Q. Gong-bin, X. Wei-wei, Geometric distortions invariant blind second generation watermarking technique based on tchebichef moment of original image, J. Software 18 (9) (2007) 2283–2294.

[13] Y. Lu, Y. Li, Y. Shen, F. Ding, X. Wang, J. Hu, S. Ding, A human action recognition method based on tchebichef moment invariants and temporal templates, in: Intelligent Human-Machine Systems and Cybernetics (IHMSC), 2012 4th International Conference on, 2, IEEE, 2012, pp. 76–79.
[14] D. Malacara, Optical Shop Testing, 59, John Wiley & Sons, 2007.
[15] R. Mukundan, Some computational aspects of discrete orthonormal moments, IEEE Trans. Image Process. 13 (8) (2004) 1055–1059.
[16] R. Mukundan, Transform coding using discrete tchebichef polynomials, in: IASTED International Conference on VIIP 2006, 2006, pp. 270–275.
[17] R. Mukundan, S. Ong, P. Lee, Discrete vs. continuous orthogonal moments for image analysis, in: International Conference on Image Science, University of Canterbury. Engineering: Conference Contributions, 2001, pp. 23–29.
[18] R. Mukundan, S. Ong, P.A. Lee, Image analysis by tchebichef moments, IEEE Trans. Image Process. 10 (9) (2001) 1357–1364.
[19] C.-Y. Pee, S. Ong, P. Raveendran, Numerically efficient algorithms for anisotropic scale and translation tchebichef moment invariants, Pattern Recognit. Lett. 92 (2017) 68–74.
[20] K.-T. Sam, X.-L. Tian, Vehicle logo recognition using modest adaboost and radial tchebichef moments, in: International Conference on Machine Learning and Computing (ICMLC 2012), 2012, pp. 91–95.
[21] R.K. Senapati, U.C. Pati, K.K. Mahapatra, Reduced memory, low complexity embedded image compression algorithm using hierarchical listless discrete tchebichef transform, IET Image Proc. 8 (4) (2014) 213–238.
[22] H. Shu, H. Zhang, B. Chen, P. Haigron, L. Luo, Fast computation of tchebichef moments for binary and grayscale images, IEEE Trans. Image Process. 19 (12) (2010) 3171–3180.
[23] D.V. Uchaev, D.V. Uchaev, V.A. Malinnikov, Chebyshev-based technique for automated restoration of digital copies of faded photographic prints, J Electron Imaging 26 (1) (2017) 011024.
[24] G. Wang, S. Wang, Recursive computation of tchebichef moment and its inverse transform, Pattern Recognit. 39 (1) (2006) 47–56.
[25] Z. Wang, A.C. Bovik, A universal image quality index, IEEE Signal Process Lett. 9 (3) (2002) 81–84.
[26] X. Yang, W. Birkfellner, P. Niederer, A similarity measure based on tchebichef moments for 2d/3d medical image registration, in: International Congress Series, 1268, Elsevier, 2004, pp. 153–158.
[27] P.-T. Yap, P. Raveendran, Image restoration of noisy images using tchebichef moments, in: Circuits and Systems, 2002. APCCAS'02. 2002 Asia-Pacific Conference on, 2, IEEE, 2002, pp. 525–528.
[28] H. Zhang, X. Dai, P. Sun, H. Zhu, H. Shu, Symmetric image recognition by tchebichef moment invariants, in: Image Processing (ICIP), 2010 17th IEEE International Conference on, IEEE, 2010, pp. 2273–2276.
[29] L. Zhang, G.-B. Qian, W.-W. Xiao, Z. Ji, Geometric invariant blind image watermarking by invariant tchebichef moments, Opt Express 15 (5) (2007) 2251–2261.
[30] H. Zhu, M. Liu, H. Shu, H. Zhang, L. Luo, General form for obtaining discrete orthogonal moments, IET Image Proc. 4 (5) (2010) 335–352.
[31] H. Zhu, H. Shu, T. Xia, L. Luo, J.L. Coatrieux, Translation and scale invariants of tchebichef moments, Pattern Recognit. 40 (9) (2007) 2530–2542.